Near wake region of an industrial scale wind turbine: comparing LES-ALM with LES-SMI simulations using data mining (POD)

IOP Conf. Series: Journal of Physics: Conf. Series **854** (2017) 012044 doi:10.1088/1742-6596/854/1/012044

Near wake region of an industrial scale wind turbine: comparing LES-ALM with LES-SMI simulations using data mining (POD)

Mandar Tabib[1], M. Salman Siddiqui[1,2], Eivind Fonn[1], Adil Rasheed[1], Trond Kvamsdal[1,2]

[1] SINTEF Digital,Mathematics and Cybernetics, Postboks 4760 Sluppen, NO-7465 Trondheim, Norway

[2] Department of Mathematical Sciences, Norwegian University of Science and Technology, NO-7491 Trondheim, Norway

E-mail: mandar.tabib@sintef.no,adil.rasheed@sintef.no

Abstract. Accurate prediction of power generation capability needs proper assessment of blade loading and wake behavior. In this regard, the Sliding Mesh Interface (SMI) approach and the Actuator Line Model (ALM) are two diverse computational fluid dynamics (CFD) based approaches of simulating the turbine behavior, each having its own merits and demerits. The SMI technique simulates the unsteady flow by explicitly modeling the blades and their rotation using a dynamic mesh, while in Actuator Line Model, the blades are not modeled explicitly but each blade is resolved as a rotating line (made of N actuator segments), over which the forces are computed. The current work focuses on simulating an industrial scale reference turbine and in differentiating the near wake dynamics predicted by these two approaches using Large Eddy Simulation (LES) and Proper Orthogonal Decomposition (POD) technique (a data mining tool). Initially, the ALM is compared with FAST model for the prediction of variation of power coefficient with the Tip Speed Ratio (TSR). The ALM is able to capture the varying trend and it predicts a similar optimum tip speed ratio as the FAST model. At this optimum TSR condition, the ALM is compared with the SMI method for a study limited to the near wake region. Comparisons between SMI and ALM shows that : (a) The SMI is predicting more complex 3D nature of the flow, and (b) the POD shows that ALM captures the shear regions of wake but it does not capture the vast compendium of length and time scales of eddies as SMI does. However, despite these limitations, the ALM has been able to capture the qualitative trend in wake deficit and the power coefficient variation with tip speed.

1. Introduction and objective

Wake dynamics have been shown to influence the power production capabilities of downstream turbines depending upon the inter-turbine distance in a wind farm layout [1–5]. Actuator Line Model (ALM) with Large Eddy Simulation (LES) turbulence model has been used popularly to understand the wake dynamics in wind farms as it is computationally tractable to do so for multi-turbine set-ups. However, it is well-known that ALM does not explicitly resolve turbine blades and hence might not be expected to be accurate enough. On the other hand, the Sliding Mesh Interface (SMI) approach resolves the blade and is expected to be more accurate but it is computationally intractable to perform for a set-up with multiple turbines. In this regard,

the current work compares the SMI and ALM methods for one industrial scale turbine. The NREL 5MW reference turbine [6] is chosen for this work, as it is a realistic and standardized industrial-scale off-shore turbine model. NREL 5 MW turbine [6] [7] consists of three $63m$ long blades defined in terms of eight cross sectional profiles (DU21, DU25, DU30, DU35, DU40 and NACA64) and twist angles at different locations away from the hub (as described in [6]). These multiple-sections with diverse angles of attack provide an ideal opportunity to test and benchmark models and methodologies that can later be applied to solve a bigger range of industrial challenges. Hence, it is popularly used by leading groups (several of USA DOEs Wind and Hydro-power Technologies Programs, EU's UpWind research program, and the International Energy Agency (IEA)'s Wind Annex XXIII Subtask Offshore Code Comparison Collaboration) to test methodologies. Such industrial scale wind-turbine blades comprising of multiple sections exhibit complex flow-patterns along the blade length [8] and generate wakes influencing wind-farm operations. In this regard, a comparison of wake dynamics and power production simulation results between sliding mesh approach (SMI) and Actuator line model will be useful to understand the comparative predictive performance of model. Thus, the objectives of this work are :

1.1. Objectives

(i) Compare the performance of ALM-LES turbulence model with FAST model in predicting power coefficient variation with varying tip speed ratio.

(ii) Compare the performance of ALM-LES turbulence model with SMI-LES approach in capturing wake dynamics at the optimum tip speed ratio.

2. Approach and Methods

The study is limited to the near wake region. The approach involves comparison of ALM and SMI approaches. Initially, the ALM is compared with FAST model for the prediction of variation of power coefficient with Tip Speed Ratio (TSR). This is done for the NREL 5 MW reference turbine. Then at the optimum TSR, ALM and SMI are compared for predicting wake structure and flow patterns. The wake dynamics simulated by SMI and ALM for the optimim $TSR = 7.5$ are compared by analyzing mean wake deficit profiles and by using Proper Orthogonal Decomposition (POD). Due to lack of experimental data of wake deficit velocity profiles for NREL 5 MW reference turbine, it is not possible to do validation of the models, so we resort to a verification exercise (i.e. comparison of different models). The governing equations and application details of SMI, ALM and POD is explained next section.

2.1. Sliding Mesh Interface (SMI) approach

The conservation equations are solved on a moving mesh (a sliding mesh) to account for the impeller motion and to capture unsteady interactions between rotating part and stationary bafes. This approach involves dividing the computational domain into a rotating and a stationary zone using a sliding interface. The approach assumes that the rotating computational mesh moves (or slides) relative to the stationary frame. The terms of the governing equations are integrated on a control volume, and the effect of the moving control volume is accounted by including the mesh motion flux in the computation of face mass flux in the convective terms (in other words the convective terms in the governing equation are modied). Thus, the face mass fluxes in the convective terms have to be computed relative to the mesh motion flux (ie. the volume swept by moving cell face during its movement with the cell face velocity). This mesh motion flux is computed based on the space (or volume) conservation law, which ensures that the moving face velocity is calculated from the face-centered positions, such that the surface vectors as well as calculation volumes inside rotating part remain constant. The mesh position in the rotating

domain is updated after every time step (as it changes with impeller rotation) and so are the cell face positions at the sliding interface. At the sliding interface, a conservative interpolation is used for both mass and momentum using a set of fictitious control volumes. The governing equations are solved only in an inertial reference frame. Following equations are solved throughout the domain for SMI approach using LES turbulence model.

$$\nabla \cdot \mathbf{u_a} = 0 \tag{1}$$

$$\frac{\partial \mathbf{u_a}}{\partial t} + \nabla \cdot (\mathbf{u_a} \otimes \mathbf{u_a}) = -\nabla p + \nabla \cdot (\nu + \nu_t)\nabla(\mathbf{u_a} + (\nabla \mathbf{u_a})^{\mathbf{T}}) \tag{2}$$

2.2. Actuator Line Model (ALM)
The turbine is modeled using actuator line model (ALM) approach, which was first developed by Sørensen and Shen [9]. The actuator line model (Equations 3, 4 and 5) uses the velocity field input from the CFD model and outputs body force, which are used as the sink term in the momentum equation. The ALM approach resolves each blade of the turbine as a rotating line (made of N actuator segments), over which the forces are computed. The forces at each segment comprise of lift force and drag forces (Equations 3, 4), which are computed from the local relative velocity (V_{rel}), local twist angle, blade chord (c), local actuator width (w) and local angle of attack (α) at a given actuator segment. The local angle of attack is computed from the tangential and normal component of relative velocity at the segment. The lift coefficient (C_l) and drag coefficient (C_d) at each segment (in Equations 3, 4 and 5) are a function of local angle of attack, and this dependency is provided as an input (blade airfoil data) to the ALM model. The force at an actuator segment i (f_i) is a point force and it is translated on to the fluid domain as a volumetric body force (F_i) using Gaussian projection (Equation 5). The regularization parameter (ε) in Equation 5 represents the width of the Gaussian and determines the concentration of the force. Larger the parameter, more smoothed out the force is on the flow field. The negative sign in Equation 5 accounts for the fact that the force exerted by turbine on the flow field is equal and opposite to the force experienced by it due to the flow. At the location (x, y, z) of the fluid domain, the overall body force is summation of force over all N actuator segments of the turbine, where (x_j, y_j, z_j) is the location of the j^{th} segment and r_j is the distance between segment j and the fluid domain location.

$$L = \frac{1}{2} C_l(\alpha) \rho V_{rel}^2 c w \tag{3}$$

$$D = \frac{1}{2} C_d(\alpha) \rho V_{rel}^2 c w \tag{4}$$

$$F_i^T(x, y, z) = -\sum_{j=1}^{N} f_i^T(x_j, y_j, z_j, t) \frac{1}{\varepsilon^3 \pi^{3/2}} exp\left[-\frac{r_j^2}{\varepsilon}\right] \tag{5}$$

2.2.1. Numerical implementation - Computational domain, mesh and parameters The turbulence is modeled using a one-equation sub-grid scale (SGS) turbulent kinetic energy LES model for both SMI and ALM. Figure 1 shows the computational domain, mesh and suitability of mesh. The adequacy of mesh for LES Simulations can be judged through the contour of the ratio of sub-grid-scale-kinetic-energy k_{sgs} to total-kinetic-energy k_{total} (as seen in figure 1(c)-1(d)). In LES simulations, the mesh-size determines spatial filtering and establishes cut-off between resolved and unresolved (modeled sub-grid scale) parts of flow. Finer the mesh, more

part of flow is resolved and more accurate are the simulation. As per criteria of Pope (2000) [10], for a well-resolved LES, less than 20% of the total kinetic energy should be modeled sub-grid-scale part (i.e. k_{sgs}/k_{total} ratio should be less than 0.2). Figure 1(c)-1(d) shows this criteria being satisfied for ALM and for most regions in SMI case. The domain size for SMI and ALM simulations (figure 1(a) and 1(b)) are kept similar: $200m \times 120m(streamwise) \times 200m$ for SMI and $200m \times 190m(streamwisedirection) \times 200m$ for ALM. SMI uses a mesh of 8 million cell elements comprising of mostly tetrahedral cells with few layers of prismatic cells to capture the blade boundary layer region, while the ALM uses a grid of 1.5 Million cells with about 50 grid points across the rotor diameter (thus minimum grid length is about $2.5m$). This grid should be sufficient to resolve wake tip vortex [11–13]. For SMI, the blade surface has been treated as wall with no-slip boundary and employs a wall function based on Spalding's law [14] that gives a continuous kinematic viscosity profile to the wall over wide range of y^+. This is required because the average y^+ value near blade wall is 667 while the minimum y^+ value is 11 and in terms of grid size - the minimum wall normal grid size is $0.008m$ near blade. Simulations are conducted with a uniform inlet wind velocity of $9m/s$ applied on the inlet face at different TSRs. The TSR is changed by adjusting the rotational speed of the turbine while keeping the inlet wind velocity constant. At the outlet face a standard outlet boundary condition is used (fixed pressure value and zero normal gradient for rest). A free slip boundary condition is applied on the rest of the surfaces. For the actuator line method, about 40 actuator segments (i.e parameter N in equation 5) were used in the simulation. The regularization parameter (ε in equation 5)in ALM is chosen to be about two times the cube root of grid volume size in that region. This is selected so as to ensure that the force is not overly concentrated to cause numerical oscillations / solver instability, and neither does the force becomes too smoothed so as to cause no resistance to the wind flowing through the turbine. For both the cases, the LES runs are initialized from the results from Reynolds Averaged Navier Stokes (RANS) simulations. For SMI, the initial RANS results are run for a total time corresponding to about four revolutions. For ALM, the RANS results are run for $100s$ of simulation time (which corresponds to the passage of 17 revolutions of the turbine and approximately 5 times flow passage through domain at wind free stream velocity). For ALM, the LES results are run for $300s$ of simulation time

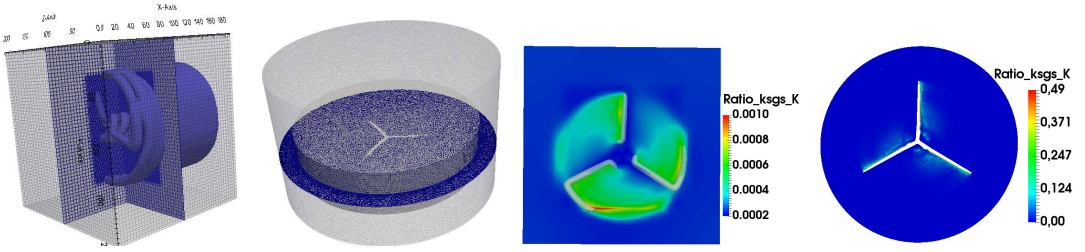

(a) ALM (b) SMI (c) ALM-Mesh Adequacy (d) SMI-Mesh Adequacy

Figure 1. Domain and Mesh information for SMI and ALM

(which corresponds to passage of 51 revolutions of turbine and approximately 14 times flow passage through domain at wind free stream velocity). The ALM simulations run at a time step of around $0.007s$ (corresponding to courant number of 0.1 which is constrained by the tip speed). The averaging was done for last $100s$. The ALM simulations are run with 16 cores on a 3.2 GHz Intel(R) Xeon (R) CPU machine and took one week of computational time. For SMI, the LES results are run for a total time of $32s$ corresponding to nearly six revolutions (and the flow developed after 4 revolutions). All the SMI LES computations are performed on 256 cores of a 2.6GHz Intel(R) Xeon(R) CPU machine on $Vilje$, the high performance computational

facility at Norwegian University of Science and Technology. The simulation time-step reached a lower value of 6e-05 s in-order to maintain the Courant number of 1. The simulation took around 3 weeks of computational time on the $Vilje$. Regarding solver, OpenFOAM was used for both SMI and ALM simulations. The equations are solved in a segregated manner using the Semi-Implicit Method for Pressure-Linked Equations (SIMPLE) algorithm. In this work, all the equations (except k_{sgs}) use second order linear convection discretization scheme. Similarly, the gradient term computation at cell faces accounts for both the orthogonal and the non-orthogonal parts.

2.3. Proper Orthogonal Decomposition (POD)

For the computation of the POD modes two dimensional snapshots of any variable (velocity components here) is required. The N snapshots are represented by $\mathbf{U} = [\mathbf{u^1}, \mathbf{u^2} \cdots \mathbf{u^N}]$ which is used to compute the covariance matrix given by $\mathbf{C} = \mathbf{U^T U}$. After this an eigenvalue problem $\mathbf{C A}^i = \lambda_i \mathbf{A}^i$ is solved to obtain the eigenvalues λ^i and eigen vectors $\mathbf{A}^i$ which are sorted in a decreasing order as $\lambda_1 > \lambda_2 > \cdots > \lambda_N$. POD modes are then computed as

$$\phi^i = \frac{\sum_{n=1}^{N} A_n^i \mathbf{u}^n}{|| \sum_{n=1}^{N} A_n^i \mathbf{u}^n ||}, i = 1, \cdots, N \tag{6}$$

With POD modes arranged as $\Psi = [\phi^1 \phi^2 \cdots \phi^N]$. POD coefficients a_i can be found from the snapshot n as $\mathbf{a}^n = \Psi^T \mathbf{u}^n$. From this a snapshot can be reconstructed as $\mathbf{u}^n = \Psi \mathbf{a}^n$. Relative energy given by any i^{th} mode is given by $\lambda_i / \sum_{j=1}^{N} \lambda_j$. POD has been successfully applied to understand wake dynamics [15, 16].

3. Result and Discussion results

3.1. Verification study: Power coefficient (C_p) Vs tip speed ratio(TSR)

For the NREL 5 MW turbine, Jonkman et.al. ([6]) studied the evolution of the power coefficient as a function of the TSR and blade-pitch surface by running FAST [17] with AeroDyn simulations. From these simulations, they found that the peak power coefficient of 0.482 occurred at a TSR of 7.55 and a rotor-collective blade-pitch angle of 0.0°. Similar study was carried out by Rannam Chaaban (data available at https://wind.nrel.gov/forum/wind/viewtopic.php?t=582) and he predicted the optimum C_p to occur at $TSR = 8$. Furthermore. Rannam's study has been used for the verification of our ALM and SMI model in Figure 2. The ALM method follows a similar trend and gives optimum power coefficient at a the TSR of 7.5 but it over-predicts the optimum power coefficient value (around 0.56). Figure 2 shows a comparison between the variation in power coefficient predicted by ALM and FAST methods. It is possible to obtain similar results as FAST by tuning regularization parameter ϵ. However, this is not done in the current work as it's a verification exercise and not a validation exercise, and all models can differ from the exact experimental observation (which are currently not available for NREL 5 MW reference turbine). The SMI method predicts a $C_p = 0.54$ at $TSR = 7.5$. The next verification is done for wind deficit.

3.2. Wake dynamics with tip speed ratios

The ALM has also been used to compare the impact of TSR on mean wind deficit (figure 4). Figure 4 compares normalized mean wind deficit $(\Delta U/U_{inflow}) = (U_{inflow} - U)/U_{inflow}$ variations at four locations downstream of the turbine ($0.3R, 0.45R, 0.9R$ and $1.3R$, where R stands for the radius of turbine $= 63m$). In all the four figures, the wind deficit at $TSR = 7.5$ is higher in the region $1.1 > z/R > 0.1$ as compared to $TSR = 9$ and $TSR = 6$. The lowest wind deficit values $(\Delta U/U_{inflow})$ in the region $(1.1 > z/R > 0.1)$ at all the four downstream locations is for $TSR = 6$. This could be explained on the basis of the energy extraction by the turbine. At

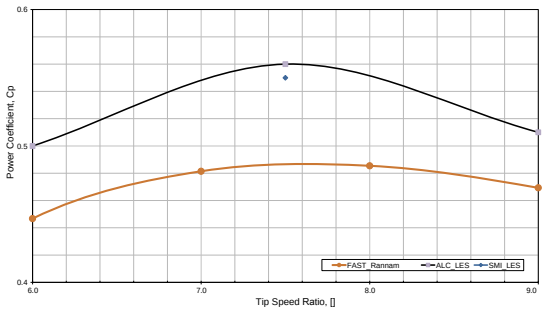

Figure 2. Verification - power coefficient versus tip speed ratio for ALM, SMI and FAST.

an optimum TSR of 7.5, more energy is extracted by the blades in that region leading to higher wind deficit and also higher C_p, while as we increase or decrease the tip speed ratio (towards 9 or 6), the energy extracted is lesser resulting in lower wind deficit and lower C_p. The wake deficit by SMI for TSR 7.5 is compared with ALM in (figure 4), and it differs in two ways, firstly SMI predicts a higher wind deficit in the near hub region ($0.1 > z/R$) at locations $0.3R$, $0.9R$ and $1.3R$ downstream of turbine. This is because the hub is explicitly modeled in case of SMI, whereas in ALM, the hub region experiences higher wind velocity and a lower negative wind deficit ($0.1 > z/R$), secondly in regions near tip vortex ($0.9R > z/R > 1.1$), ALM shows a sharp velocity gradient corresponding to the presence of shear region accompanying tip vortex and it shows higher wake velocity deficit in the core wake region ($0.2R > z/R > 0.9$). Either, it could be because of higher turbulence that the wakes are decaying faster in SMI or because of mesh size. Despite these differences in wake velocity deficit, the power coefficient in SMI is slightly lower than ALM because higher energy gets extracted at the tip edge region (which produces most of the torque) which compensates for the lower energy extracted at the core wake region in SMI, as compared to the ALM case.

Figure 3 compares the flow structures and flow pattern captured by SMI and ALM Approach. The wake structures obtained in the near wake region by SMI and ALM are shown in figure 3(a) and in figure 3(d) respectively. The vorticity contours show that both the methods (and the mesh used) are able to capture the helical wake structures downstream of blade at an altitude along the periphery of blade tip. A higher vorticity region is captured by SMI at regions downstream at altitude between the tip periphery and root, which could be because of a chaotic flow induced in this region by explicit rotating blade of SMI as shown in streamlines (figure 3(e)). Figure 3(b) and figure 3(e) compares the flow path (streamlines) predicted by SMI and ALM, with streamlines colored by magnitude of velocity. SMI captures a higher 3D chaotic flow behavior in regions behind the turbine as compared to the ALM (which does not show this much chaotic 3D flow). Further, the highest velocity in ALM streamline is about 11 m/s while SMI streamline captures a highest velocity (65 m/s) almost equivalent to the blade tip speed ($\omega r = 1.071 * 63 = 67.4 m/s$), which could be due to non-slip boundary on the rotating blade geometry in SMI. For sake of comparison, the color-bar range for streamlines is set at the highest velocity magnitude captured by the SMI. Further, figure 3(c) and figure 3(f) shows the flow pattern at the DU40 segment (located near the hub) in terms of mean velocity vectors captured by the SMI and ALM respectively. In figure 3(f), the velocity vectors colored by velocity magnitude is imposed on a pressure contour. At TSR 7.5, SMI shows the wind approaching the blade at an angle of attack and the explicit rotating bluff body airfoil segment has major influence on the velocity vector direction and magnitude as it crosses the blade, while with ALM, the velocity vectors seemed to only deviate slightly as it crossed the similar blade region (note that ALM do not have explicit blade and this DU40 region was identified using

vorticity iso-surface). The flow vector differences can be attributed to the distributed nature of force projection in ALM methodology along with the non-explicit resolution of blade. However, despite these limitations, ALM has been able to predict the trends in wake deficit and power coefficients. Thus, the performance of ALM method is compared with the SMI model. The impact of these two diverse methodologies on wake dynamics is further captured by POD as described in section 3.3 below.

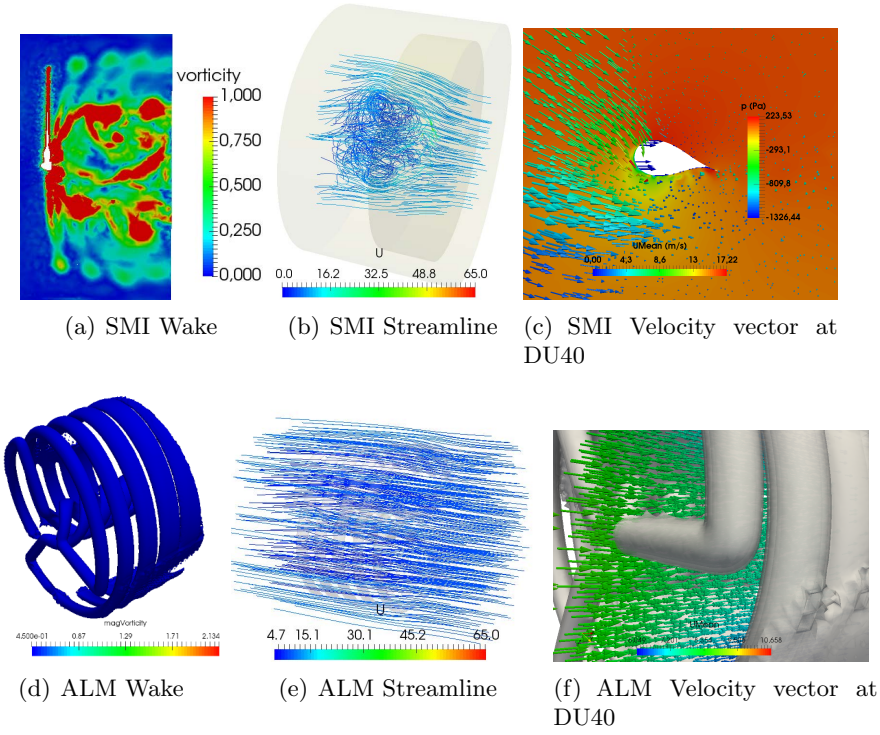

(a) SMI Wake (b) SMI Streamline (c) SMI Velocity vector at DU40

(d) ALM Wake (e) ALM Streamline (f) ALM Velocity vector at DU40

Figure 3. Impact of tip speed ratio (TSR) on flow pattern

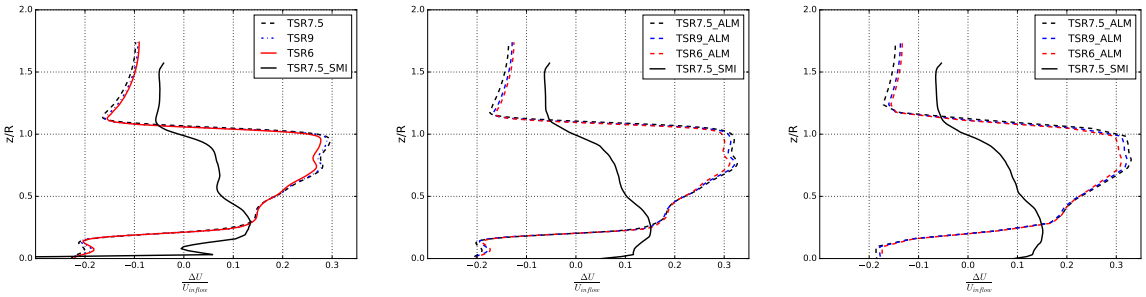

(a) 0.3R distance behind turbine (b) 0.9R distance behind turbine (c) 1.3R distance behind turbine

Figure 4. Verifying impact of tip speed ratio on normalized mean velocity deficit.

3.3. POD comparison

To conduct POD the simulation data from ALM and SMI was first interpolated onto a rectilinear grid. For ALM, the data sampled at 7 Hz, is interpolated on a uniform rectilinear grid measuring

380×400 elements, with a grid-size of $0.5m \times 0.5m$. The POD is applied on 720 planes over a total time of $100s$. For SMI, the data sampled at 166 Hz, is interpolated on a uniform rectilinear grid measuring 240×400 elements, with a grid-size of $0.5m \times 0.5m$. The POD is applied on 1000 planes over a total time of $6s$ (corresponding to nearly one rotation). It is ensured that most of the flow realizations are captured in the samples used for conducting the POD. Figure 6 and figure 7 shows the contours of decomposed velocity modes. Their values do not physically represent the velocity. These values represent distribution of energy content in the mode, and gives idea about overall energy captured by the mode and the flow structure associated with it. High values (red color regions) signifies higher energy content and blue color regions signifies lower energy content. The color bars are not relevant to the study here and are not shown, only the total energy captured by a mode and associated flow structure is relevant. Figure 6

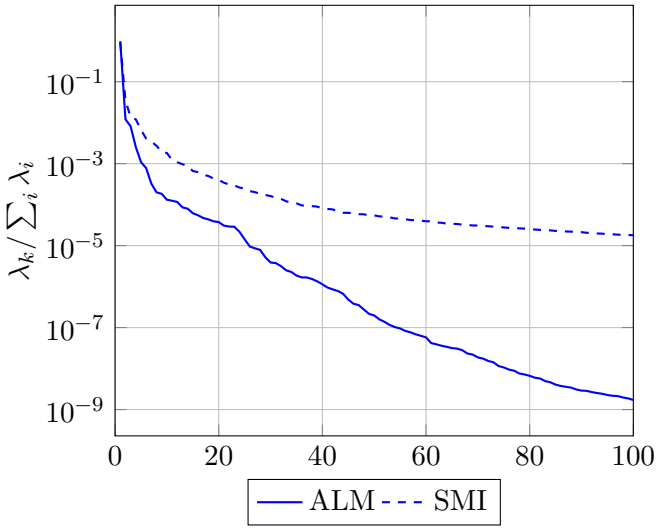

Figure 5. Energy spectra of SMI and ALM simulations

gives the flow structures represented by the first four modes for the ALM simulations conducted for at $TSR = 7.5$. It can be seen from the figure that the first mode represents the most energetic (97.5% of the total energy) and probable realization of the flow which looks like the mean wind field. As we move to higher modes we discover that the associated energy decrease rapidly. Together, the first three modes account for 99.5% of the total energy. The spatial scales associated with flow structures also decrease. It is also clear from the figures that the first four modes capture distinct kinds of flow structures hinting at a clear scale separation at least in space. On the other hand, in the case of SMI, the first mode corresponds to only 90% of the total energy. It hints at a spreading of the larger flow structures to higher modes. The explicit churning motion of the blades generate large eddies (Figure 7) which break down into smaller eddies and no clear scale separation is observed when compared to the ALM simulation as a result of which the energy drop across modes is more gradual. However, together the first 30 modes capture 99.5% of the total energy. The need for slightly more number of modes in the case of SMI suggests that it is able to capture flow with more unsteadiness and wider range of spatio-temporal scales either owing to explicit blade resolution or perhaps the faster decay of wakes through the energy cascading process (and hence there are more length and time scales in the given domain). It is worth highlighting here that although the effects of hub vortex is quantitatively captured using both the approach, the same is not true for the tip-vortices. A reasonable explanation can be that the current POD is conducted on 2D snapshots where the tip

vortices are only represented as dots contributing very little energy compared to the other flow structures. In order to capture the helical tip vortices, POD using three dimensional field should be conducted. This was not possible during the course of this work but remains an investigation for the future.

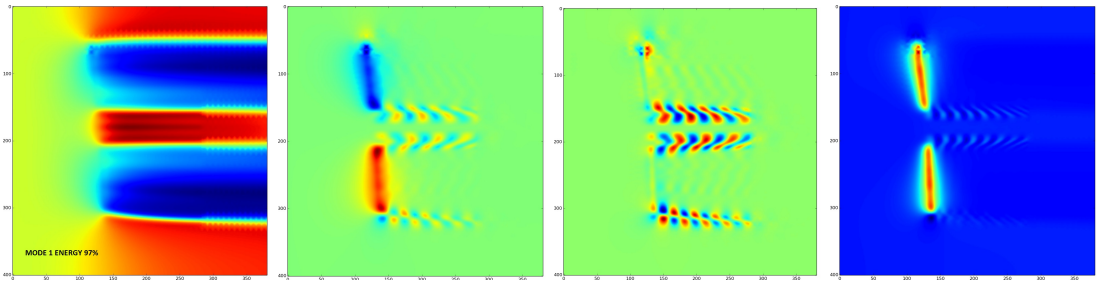

(a) Mode1 Energy 97% (b) Mode2 Energy 1.21% (c) Mode3 Energy 0.8% (d) Mode4 Energy 0.2%

Figure 6. First four modes extracted from the ALM simulations using POD. Contours of Decomposed velocity modes.Red color region represents high values and blue color region represents low values.

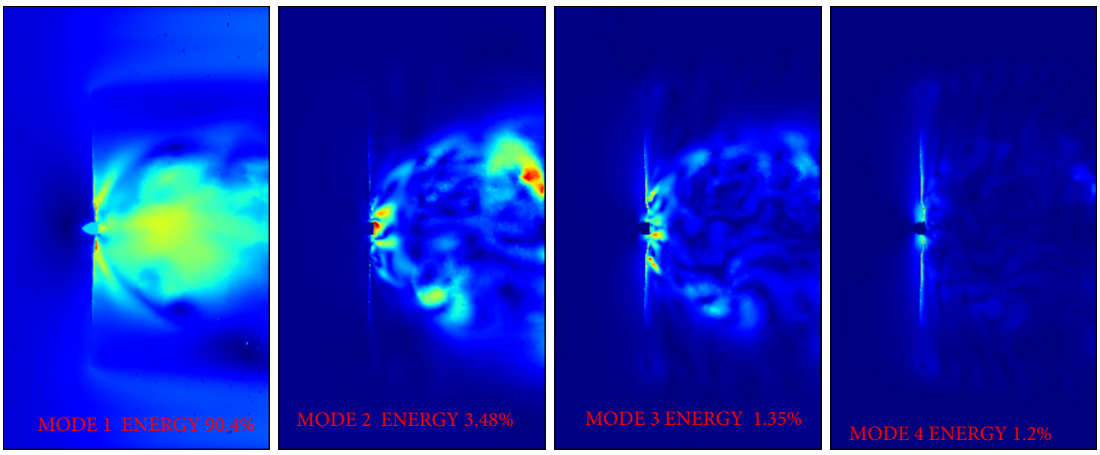

Figure 7. First four modes extracted from the SMI simulations using POD.Contours of Decomposed velocity modes.Red color region represents high values and blue color region represents low values.

4. Conclusion and future work

The paper aims to use LES and POD technique to differentiate wake dynamics captured by two diverse methods (ALM and SMI techniques) for an industrial scale wind turbine. The paper has been able to show that:

- ALM method is compared with the FAST model in its ability to compute power coefficient with varying tip speed ratios for an industrial scale turbine, and ALM is able to capture the trend in a similar way as FAST.
- The POD analysis also reveals that SMI has been able to capture a compendium of eddies with variable time scales. As a result, its first mode is not as dominant (90% of energy) as

the first mode from ALM (which captures 97% of energy). The ALM first mode shows the shear along the tip periphery and hub periphery dominantly and most energy lies in this mode itself, while the rest of structures (scales) have less energy and are in the remaining modes.

- A comparison in prediction of flow-pattern and wake structure by ALM and SMI shows that the SMI predicts a more complex 3D nature of flow. Despite these differences, the ALM has been able to follow the qualitative trend in wake deficit and power coefficient variation with tip speed, owing to the line source and the distributed nature of force projection. The current work is focussed on near wake region study. In future, it will be interesting to study the wakes further downstream.

Acknowledgments

The authors acknowledge the financial support from the Norwegian Research Council and the industrial partners of NOWITECH: Norwegian Research Centre for Offshore Wind Technology (Grant No.:193823/S60) (http://www.nowitech.no) and FSI-WT (Grant No.:216465/E20)(http://www.fsi-wt.no).

References

[1] Churchfield M, Lee S, Moriarty P, Martnez L, Leonardi S, Vijayakumar G and Brasseur J 2012 *50th AIAA Aerospace Sciences Meeting Including the New Horizons Forum and Aerospace Exposition* 124 (2) 393–399
[2] Porté-Agel F, Wu Y, Lu H and Conzemius R 2011 *Journal of Wind Engineering and Industrial Aerodynamics* 99(4): 154–168
[3] Tabib M V, Rasheed A, and Kvamsdal T 2015 *Journal of Physics: Conference Series* 625: 012032
[4] Tabib M V, Rasheed A and Fuchs F 2016 *Journal of Physics: Conference Series* 753 (3), 032063
[5] Tabib M V, Rasheed A, and Kvamsdal T 2015 *Energy Procedia, 80* 302311
[6] Jonkman J, Butterfield S, Musial W and Scott G 2009 *National Renewable Energy Laboratory* **Tech. Rep. NREL/TP-500e38060**
[7] Kooijman H, Lindenburg C, Winkelaar D and Hooft E 2003 *DOWEC Dutch Offshore Wind Energy Converter 1997-2003 Public Reports , DOWEC 10046-009, ECN-CX–01-135, Petten, the Netherlands: Energy Research Center of the Netherlands*
[8] Tabib M V and Rasheed A 2017 *EERA Deepwind Conference, Trondheim*
[9] Sørensen J and Shen W 2002 *Journal of Fluids Engineering* 124 (2) 393–399
[10] Pope S 2000 *Cambridge University Press*
[11] Troldborg N, Sorensen J and Mikkelsen R 2010 *Wind Energy* **13** 86–99
[12] Martinez L, Leonardi S, Churchfield M and Moriarty P 2012 A comparison of actuator disk and actuator line wind turbine models and best practices for their use
[13] Jha P, Churchfield M, Moriarty P and Schmitz S 2014 *Journal of Solar Energy Engineering, Transactions of the ASME* **136**
[14] Spalding D 1961 *Transactions ofth ASIDE, Series E: Journal of Applied Mechanics* 28,455–458
[15] Bastine D, Witha B, Wchter M and Peinke J 2014 *Journal of Physics: Conference Series* **524**
[16] Braud C, Heitz D, Braud P, Arroyo G and Delville J 2004 *Experiments in Fluids* **37** 95–104
[17] Jonkman J, Marshal L and Buhl J 2005 *National Renewable Energy Laboratory, Golden, CO,* **Tech. Rep. NREL/EL-500-38230**